

This discussion paper is/has been under review for the journal Atmospheric Measurement Techniques (AMT). Please refer to the corresponding final paper in AMT if available.

GOMOS bright limb ozone data set

S. Tukiainen¹, E. Kyrölä¹, J. Tamminen¹, and L. Blanot²

¹Finnish Meteorological Institute, Earth Observation Unit, Helsinki, Finland

²ACRI-ST, Sophia Antipolis, France

Received: 5 December 2014 – Accepted: 13 January 2015 – Published: 27 January 2015

Correspondence to: S. Tukiainen (simo.tukiainen@fmi.fi)

Published by Copernicus Publications on behalf of the European Geosciences Union.

AMTD

8, 987–1011, 2015

GOMOS bright limb data set

S. Tukiainen et al.

Title Page	
Abstract	Introduction
Conclusions	References
Tables	Figures
◀	▶
◀	▶
Back	Close
Full Screen / Esc	
Printer-friendly Version	
Interactive Discussion	



Abstract

We have created a daytime ozone profile data set from the measurements of the Global Ozone Monitoring by Occultation of Stars (GOMOS) instrument on board the Envisat satellite. This so-called GOMOS bright limb (GBL) data set contains $\sim 358\,000$ stratospheric daytime ozone profiles measured by GOMOS in 2002–2012. The GBL data set complements the widely used GOMOS night-time data based on stellar occultation measurements. The GBL data set is based on the GOMOS daytime occultations but instead of the transmitted star light, we use limb scattered solar light. The ozone profiles retrieved from these radiance spectra cover 18–60 km tangent height range and have approximately 2–3 km vertical resolution. We show that these profiles are generally in better than 10 % agreement with the NDACC (Network for the Detection of Atmospheric Composition Change) ozone sounding profiles and with the GOMOS night-time, MLS (Microwave Limb Sounder), and OSIRIS (Optical Spectrograph, and InfraRed Imaging System) satellite measurements. However, there is a 10–13 % negative bias at 40 km tangent height and a 10–50 % positive bias at 50 km when the solar zenith angle $> 75^\circ$. These biases are most likely caused by stray light which is difficult to characterize and remove entirely from the measured spectra. Nevertheless, the GBL data set approximately doubles the amount of useful GOMOS ozone profiles and improves coverage of the summer pole.

20 1 Introduction

The GOMOS (Global Ozone Monitoring by Occultation of Stars) instrument on board the Envisat satellite use stellar occultation technique for monitoring ozone and other trace gases in the middle atmosphere (Bertaux et al., 2010). Envisat operated from 2002–2012 and during that time GOMOS measured altogether around 880 000 occultations. While the GOMOS night-time ozone profiles have generally smaller than 5 % bias in the stratosphere (Meijer et al., 2004; van Gijsel et al., 2010; Kyrölä et al., 2013),

AMTD

8, 987–1011, 2015

GOMOS bright limb data set

S. Tukiainen et al.

[Title Page](#)

[Abstract](#)

[Introduction](#)

[Conclusions](#)

[References](#)

[Tables](#)

[Figures](#)

◀

▶

◀

▶

[Back](#)

[Close](#)

[Full Screen / Esc](#)

[Printer-friendly Version](#)

[Interactive Discussion](#)



majority of the daytime occultation profiles are poor due to weak signal to noise ratio (Verronen et al., 2007). For this reason, the GOMOS daytime occultation profiles have not been used in scientific studies.

To improve the GOMOS daytime ozone profiles, Taha et al. (2008) suggested using atmospheric limb radiance of scattered sunlight instead of star spectra for the daytime retrievals. GOMOS measured limb radiances above and below the occulting star using a separate optical path so that the star and the limb contributions could be distinguished from each other (see Bertaux et al., 2010, for detailed description of the instrument). In principle, the subtraction of the pure limb signal from the central band, containing both the star and the limb contribution, should produce an uncontaminated star spectrum. However, it seems that this removal is leading to large and poorly understood uncertainties in the daytime transmission spectra, ruining the operational GOMOS occultation retrieval that works fine for the night-time data.

Following the promising early results of Taha et al. (2008), Tukiainen et al. (2011) developed an alternative method for retrieving ozone profiles from the GOMOS limb scattered radiances, or GOMOS bright limb (GBL) measurements as they are referred now on. This paper is a continuation of that study. We have processed all GOMOS daytime measurements and in this study we estimate the quality of this novel data set. The structure of this paper is as follows. In Sect. 2 we describe the retrieval method and explain some general aspects of the GOMOS daytime data. In Sect. 3 we describe the correlative data sets used to validate the retrieved GBL ozone profiles, present the comparison method, and show the results of the comparisons. In Sect. 4 we conclude our study and discuss the results.

2 GOMOS bright limb data

The GOMOS bright limb data set consists of ~ 358 000 limb scattered daytime radiance spectra measured between March 2002 and April 2012, from the launch of Envisat to the communication failure that stopped the mission. From these measurements we

GOMOS bright limb data set

S. Tukiainen et al.

[Title Page](#)

[Abstract](#)

[Introduction](#)

[Conclusions](#)

[References](#)

[Tables](#)

[Figures](#)

[◀](#)

[▶](#)

[Back](#)

[Close](#)

[Full Screen / Esc](#)

[Printer-friendly Version](#)

[Interactive Discussion](#)



have retrieved vertical ozone profiles in the 18–60 km altitude range. The retrieved profiles have approximately 2–3 km vertical resolution. The data are processed using the ESA IPF Level 1 version 6.01 and the current GBL Level 2 version 1.2. The Level 2 retrieval scheme is based on Tukiainen et al. (2011) with a few modifications. We describe the retrieval method briefly below.

One GOMOS limb “scan” includes typically 120–140 individual radiance measurements at different tangent heights. Or actually twice as much because, as already mentioned, GOMOS records two separate radiance spectra at each tangent height, above and below the central band (which collects the combined star and limb signal).

The GBL data set was processed using the lower band radiances but the upper band, or possibly a combination of both bands, could be used as well. The upper and lower band radiances are separated by around 1.5 km in tangent height. One particular advantage of GOMOS is that the tangent height registration is very accurate. Stars are point sources and their positions are well known. The uncertainty in the tangent height, which is often a significant problem in limb scatter satellite observations, is a negligible issue in the GOMOS retrievals (Tamminen et al., 2010).

In the retrieval, the atmosphere is discretized so that each of these radiance measurements is assumed to characterize a homogeneous layer. We use an onion peeling retrieval approach to estimate trace gas densities starting from the topmost layer used in the retrieval (at ~60 km) and proceeding layer by layer towards the bottom layer (at ~18 km). At each layer, we minimize the cost function

$$\chi^2(z) = [\mathbf{H}(\lambda, z) - \mathbf{M}(\lambda, z)]\mathbf{C}^{-1}[\mathbf{H}(\lambda, z) - \mathbf{M}(\lambda, z)]^T, \quad (1)$$

where \mathbf{M} is the (stray light corrected) radiance measurement at layer z and a function of wavelength λ . It is normalized with the first measurement below 47 km of the same scan. The diagonal uncertainty covariance matrix \mathbf{C} includes the standard deviation of the measurement error. Currently, no modeling error is assumed, see details

GOMOS bright limb data set

S. Tukiainen et al.

Title Page	
Abstract	Introduction
Conclusions	References
Tables	Figures
	
	
Full Screen / Esc	
Printer-friendly Version	
Interactive Discussion	



$$H(\lambda, z) = R(\lambda, z) \frac{I_{ss}(\lambda, z, \rho)}{I_{ref}(\lambda)} \quad (2)$$

consists of the modeled total to single scattering ratio R and the single scattering radiance I_{ss} divided by the modeled reference spectrum I_{ref} . The retrieved gas densities ρ include ozone, aerosols, and neutral air. NO₂ is taken from a climatology and kept fixed. The NO₂ climatology is based on OSIRIS data (Tukiainen et al., 2008). Aerosol scattering is modeled with the Henyey–Greenstein phase function and aerosol extinction is modeled with the well known Ångstrom's λ^{-1} law. Rayleigh scattering is assumed for neutral air. The minimization of χ^2 in Eq. (1) is done with the Levenberg–Marquardt method.

GOMOS daytime radiances are significantly contaminated by stray light, especially at visible wavelengths and at high tangent altitudes. For example, below 40 km at 500 nm the stray light accounts roughly a few percents of the signal but already several tens of percents at 60 km. We remove the stray light by calculating the average spectrum above 100 km and by subtracting this constant spectrum from each tangent height. The removal is done independently for each scan. This approach ignores possible altitude dependence of the stray light but on the other hand is a simple and robust method. To avoid using the most corrupted wavelength regions, we use three different sets of retrieval wavelengths depending on the tangent height (Table 1). This reduces bias due to inconsistencies in the GOMOS spectra but also introduces a discontinuity at 40 km where we start using only visible wavelengths. We reduce the discontinuity by scaling the amount of stray light (at layers below 40 km) by an iteratively found constant factor, requiring that the ozone profile remains smooth in the 40 km transition.

We tested the sensitivity of the GBL ozone to the two important assumptions in the retrieval: the choice of the CCD band (upper or lower) and the stray light correction method. The test data included 10 orbits (142 scans) from 1 April 2004. The two available CCD bands yield ozone profiles within 1 % (Fig. 1 left panel). The difference is

GOMOS bright limb
data set

S. Tukiainen et al.

Title Page

Abstract

Introduction

Conclusions

References

Tables

Figures

◀

▶

◀

▶

Back

Close

Full Screen / Esc

Printer-friendly Version

Interactive Discussion



**GOMOS bright limb
data set**

S. Tukiainen et al.

calculated, after linear interpolation in altitude, as $(\text{upper-lower})/\text{lower} \times 100 [\%]$. This figure visualizes the propagation of the random measurement error in the GOMOS limb retrieval. For the stray light correction, we tested two methods: the constrained extrapolation method introduced in Tukiainen et al. (2011) and the simple average method described above. The difference in the retrieved ozone profiles is below 1 % (Fig. 1 right panel). The difference is defined as $(\text{average-constrained})/\text{constrained} \times 100 [\%]$. As both methods produce, at least in this case, almost identical ozone profiles it is probably better to use the average method because of its simplicity.

Each GBL Level 2 file contains geolocation information, ECMWF model values for the temperature and density, fixed NO_2 profile (from the OSIRIS climatology), and residuals of the fit. Densities and error estimates are provided for the three simultaneously retrieved species: ozone, aerosols, and neutral air. In this paper we show only the results related to the ozone profiles. Figure 2 shows the number of GBL profiles and GOMOS night-time occultation profiles during the whole Envisat mission. The GBL data set roughly doubles the amount of useful GOMOS ozone profiles. Figure 3 shows a typical one day coverage of GOMOS day and night measurements, and Fig. 4 shows the number of GBL profiles during one year (2004) as a function of latitude. The GBL data complements the night occultations in the tropics and mid latitudes and furthermore expands the global coverage towards the summer pole.

Figure 5 shows an example of the zonally averaged vertical distribution of ozone from the GOMOS night-time occultations, GOMOS daytime occultations, and GBL. The measurements are from January 2005 and from the latitude 35°N . The night-time data are from the star number 2 and the daytime data from the star number 175. As practically always, the shapes of the day occultation profiles are significantly different than the shapes of the GBL and night occultation profiles. The huge fluctuations and large negative values seen in the day occultation profiles are not realistic. At least in the stratosphere, the quality of the day occultation profiles is clearly inferior to the GBL and GOMOS night-time data.

Title Page	
Abstract	Introduction
Conclusions	References
Tables	Figures
	
	
Full Screen / Esc	
Printer-friendly Version	
Interactive Discussion	



3 Correlative data sets

GOMOS bright limb data set

S. Tukiainen et al.

Title Page

Abstract

Introduction

Conclusions

References

Tables

Figures

◀

▶

◀

▶

Back

Close

Full Screen / Esc

Printer-friendly Version

Interactive Discussion



OSIRIS is an UV/Visible spectrograph, including a near infrared imager, on board the Odin satellite. OSIRIS measures the atmosphere using the limb scatter technique, measuring scattered sunlight and scanning the Earth's limb between $\sim 10\text{--}100\text{ km}$. There are at least two different OSIRIS Level 2 ozone products available. Widely used and extensively validated ozone product is produced by the University of Saskatchewan (e.g., Adams et al., 2012, 2013). In this paper we used the Saskatchewan Level 2 version 5.07 data. We also used another OSIRIS Level 2 ozone product processed by the Finnish Meteorological Institute (Tukiainen et al., 2008). The current version of the FMI's OSIRIS data is 3.2. The FMI's OSIRIS data is retrieved with a similar type inversion method than is used in this study with the GOMOS data.

3.1 Comparison method

For each co-located profile pair we calculated the difference as

$$\Delta = \frac{X_{\text{GBL}} - X_{\text{ref}}}{X_{\text{ref}}} \times 100 [\%], \quad (3)$$

where X_{GBL} is a GBL profile and X_{ref} is a reference (NDACC, GOMOS night, MLS or OSIRIS) profile. The coincidence criteria for each instrument are shown in Table 3. To estimate the bias against GOMOS night, MLS and OSIRIS, we calculated the median of the individual relative differences using 10° latitude zones between 70°S and 70°N . With the NDACC soundings we used only six latitude zones (see Table 2) because the latitude coverage of the NDACC sounding stations is much sparser than of the polar orbiting satellites especially in the Southern Hemisphere. We also calculated the bias against GOMOS night occultations as a function of solar zenith angle.

In the median calculation, we used coincidences from all overlapping years. Possible year-to-year differences due to aging of the instruments etc. were found insignificant (a few percents with no clear pattern) compared to the other sources of bias. In addition, the vertical resolutions of the four different satellite ozone products are similar (2–3 km for GBL, GOMOS night, and OSIRIS, and $\sim 3\text{ km}$ for MLS). Therefore, these profiles

**GOMOS bright limb
data set**

S. Tukiainen et al.

[Title Page](#)[Abstract](#)[Introduction](#)[Conclusions](#)[References](#)[Tables](#)[Figures](#)[◀](#)[▶](#)[Back](#)[Close](#)[Full Screen / Esc](#)[Printer-friendly Version](#)[Interactive Discussion](#)

were compared without any vertical smoothing. The NDACC ozone sounding profiles were smoothed to the approximately same resolution with a Gaussian filter.

Some of the GBL profiles include outliers especially at the lowermost retrieved tangent height. This measurement is often corrupted because GOMOS has lost the tracking of the star. Before comparisons we screened the GBL data with the following criteria:

1. Always remove the lowest retrieved point,
2. Remove points with the reduced $\chi^2 > 10$,
3. Remove points below 35 km where the relative error $\frac{O_3(\text{error})}{O_3(\text{density})} > 0.1$, where $O_3(\text{error})$ is the error estimate of the retrieved density

This kind of screening significantly improves the agreement in the 20–25 km range against all studied reference data.

3.2 Results

Figure 6 shows the result against NDACC soundings for the six latitude zones. Shown are interquartile ranges and medians of the differences. The numbers represent the numbers of co-located pairs at each tangent height. In these comparisons the median difference is always less than 10 % except latitudes 60–90° S where the negative bias is more than –20 % at 19 km.

Figure 7 shows the comparison against GOMOS night occultation for different solar zenith angles. There is a clear positive bias at around 50 km when the solar zenith angle is 75° or larger. With smaller solar zenith angles the differences are rather similar. The large solar zenith angle observations account for 16 % of the GBL data and the GOMOS measurement geometry is such that these observations appear mostly at mid and high latitudes. We suspect that the 50 km bias is linked to stray light and its removal. GOMOS daytime data suffer from serious stray light contamination and particularly the

upper altitudes are sensitive to the accuracy of the removal method. Because the GBL measurements with a large solar zenith angle are distinctly biased at 50 km, in the remaining comparisons we only used the GBL data with the solar zenith angle smaller than 75°.

- 5 Figure 8 shows the difference in 10° latitude bins against GOMOS night, MLS, and OSIRIS measurements. The most distinctive feature is the 10–15 % negative bias at around 40 km, which is present in all comparisons. A few percent of this difference can be explained by the diurnal variation of ozone. The GOMOS day measurements are made around 10 a.m. LT which is in the minimum of the diurnal curve (Sakazaki et al.,
10 2013). In addition, the MLS afternoon measurements are made around 2 p.m., which is in the quite recently discovered afternoon maximum of ozone. We estimate that the diurnal variation explains about 3 % of the 40 km bias against MLS and around 1–2 % against GOMOS night-time and OSIRIS. Another notable structure is the negative bias
15 at Southern mid/high latitudes, which is tens of percents at 19 km. Large biases exist at tropic/sub tropic region below 21 km but the deviations are large, too. Remaining differences are below 10 % (and often < 5 %).

4 Discussion and summary

- We have processed and released a GOMOS bright limb ozone data set. This data set roughly doubles the number of useful GOMOS ozone profiles. In general, the bias
20 in the GBL ozone is less than 10 %, and often less than 5 %, but there is a clear 10–13 % negative bias at 40 km. The reason for this bias is uncertain but the most likely cause is the stray light contamination in the 300–320 nm band already noted by Tukiainen et al. (2011). Above the 45 km tangent height we use UV wavelengths to retrieve ozone and below 40 km we use visible wavelengths. The retrieval method is
25 sensitive to the transition from UV to visible and it is easily disturbed by stray light. As explained above, we scale the amount of stray light to get smooth ozone profile in the 40 km transition. This ad-hoc approach works reasonably well in practice but better

GOMOS bright limb data set

S. Tukiainen et al.

[Title Page](#)

[Abstract](#)

[Introduction](#)

[Conclusions](#)

[References](#)

[Tables](#)

[Figures](#)

◀

▶

[Back](#)

[Close](#)

[Full Screen / Esc](#)

[Printer-friendly Version](#)

[Interactive Discussion](#)



ways to switch between the different wavelength domains should be investigated in future.

The diurnal variation explains about 1–3 % of the observed 40 km bias as the GO-MOS day measurements are made during the minimum of the diurnal cycle. At the 5 50 km tangent altitude we have up to 50 % positive bias depending on the solar zenith angle. This bias can not be explained by natural variation. It indicates some problem in the retrieval, most likely related to the stray light and its correction. Until this issue is solved, it is recommended to only use GBL measurements with the solar zenith angle less than 75° when using data from the tangent heights above 45 km.

10 The GBL Level 2 files are available from the [ftp.fmi.fi](ftp://ftp.fmi.fi) server with the username gomosGBL and password kOs20mos!. The file format is HDF5 (one file for each profile) and the total size of the whole data set is about 22 GB.

Acknowledgements. This study was funded by the European Space Agency through the SPIN project (<http://esa-spin.org>) and by the Academy of Finland through the MIDAT project. The 15 authors appreciate MLS and OSIRIS teams for sharing their data and Viktoria Sofieva for commenting the manuscript. The (ozone sounding) data used in this publication were obtained as part of the Network for the Detection of Atmospheric Composition Change (NDACC) and are publicly available (see <http://www.ndacc.org>).

References

20 Adams, C., Strong, K., Batchelor, R. L., Bernath, P. F., Brohede, S., Boone, C., Degenstein, D., Daffer, W. H., Drummond, J. R., Fogal, P. F., Farahani, E., Fayt, C., Fraser, A., Goutail, F., Hendrick, F., Kolonjari, F., Lindenmaier, R., Manney, G., McElroy, C. T., McLinden, C. A., Mendonca, J., Park, J.-H., Pavlovic, B., Pazmino, A., Roth, C., Savastiouk, V., Walker, K. A., Weaver, D., and Zhao, X.: Validation of ACE and OSIRIS ozone and NO₂ measurements using ground-based instruments at 80° N, *Atmos. Meas. Tech.*, 5, 927–953, doi:10.5194/amt-25 5-927-2012, 2012. 994

Adams, C., Bourassa, A. E., Bathgate, A. F., McLinden, C. A., Lloyd, N. D., Roth, C. Z., Llewellyn, E. J., Zawodny, J. M., Flittner, D. E., Manney, G. L., Daffer, W. H., and Degen-

[Title Page](#)

[Abstract](#)

[Introduction](#)

[Conclusions](#)

[References](#)

[Tables](#)

[Figures](#)

◀

▶

[Back](#)

[Close](#)

[Full Screen / Esc](#)

[Printer-friendly Version](#)

[Interactive Discussion](#)



**GOMOS bright limb
data set**

S. Tukiainen et al.

[Title Page](#)[Abstract](#)[Introduction](#)[Conclusions](#)[References](#)[Tables](#)[Figures](#)[|◀](#)[▶|](#)[◀](#)[▶](#)[Back](#)[Close](#)[Full Screen / Esc](#)[Printer-friendly Version](#)[Interactive Discussion](#)

GOMOS bright limb
data set

S. Tukiainen et al.

- and Nordh, L.: The OSIRIS instrument on the Odin spacecraft, *Can. J. Phys.*, 82, 411–422, doi:10.1139/p04-005, 2004. 993
- Meijer, Y. J., Swart, D. P. J., Allaart, M., Andersen, S. B., Bodeker, G., Boyd, I., Braathen, G., Calisesi, Y., Claude, H., Dorokhov, V., von der Gathen, P., Gil, M., Godin-Beekmann, S., Goutail, F., Hansen, G., Karpetchko, A., Keckhut, P., Kelder, H. M., Koelemeijer, R., Kois, B., Koopman, R. M., Kopp, G., Lambert, J.-C., Leblanc, T., McDermid, I. S., Pal, S., Schets, H., Stubi, R., Suortti, T., Visconti, G., and Yela, M.: Pole-to-pole validation of Envisat GOMOS ozone profiles using data from ground-based and balloon sonde measurements, *J. Geophys Res.-Atmos.*, 109, 2156–2202, doi:10.1029/2004JD004834, 2004. 988
- Sakazaki, T., Fujiwara, M., Mitsuda, C., Imai, K., Manago, N., Naito, Y., Nakamura, T., Akiyoshi, H., Kinnison, D., Sano, T., Suzuki, M., and Shiotani, M.: Diurnal ozone variations in the stratosphere revealed in observations from the Superconducting Submillimeter-Wave Limb-Emission Sounder (SMILES) on board the International Space Station (ISS), *J. Geophys Res.-Atmos.*, 118, 2991–3006, doi:10.1002/jgrd.50220, 2013. 996
- Taha, G., Jaross, G., Fussen, D., Vanhellemont, F., Kyrölä, E., and McPeters, R. D.: Ozone profile retrieval from GOMOS limb scattering measurements, *J. Geophys Res.-Atmos.*, 113, 2156–2202, doi:10.1029/2007JD009409, 2008. 989
- Tamminen, J., Kyrölä, E., Sofieva, V. F., Laine, M., Bertaux, J.-L., Hauchecorne, A., Dalaudier, F., Fussen, D., Vanhellemont, F., Fanton-D'Andon, O., Barrot, G., Mangin, A., Guirlet, M., Blanot, L., Fehr, T., Saavedra de Miguel, L., and Fraisse, R.: GOMOS data characterisation and error estimation, *Atmos. Chem. Phys.*, 10, 9505–9519, doi:10.5194/acp-10-9505-2010, (2010). 990
- Tukiainen, S., Hassinen, S., Seppälä, A., Auvinen, H., Kyrölä, E., Tamminen, J., Haley, C. S., Lloyd, N., and Verronen, P. T.: Description and validation of a limb scatter retrieval method for Odin/OSIRIS, *J. Geophys Res.-Atmos.*, 113, 2156–2202, doi:10.1029/2007JD008591, 2008. 991, 994
- Tukiainen, S., Kyrölä, E., Verronen, P. T., Fussen, D., Blanot, L., Barrot, G., Hauchecorne, A., and Lloyd, N.: Retrieval of ozone profiles from GOMOS limb scattered measurements, *Atmos. Meas. Tech.*, 4, 659–667, doi:10.5194/amt-4-659-2011, 2011. 989, 990, 991, 992, 996
- Waters, J. W., Froidevaux, L., Harwood, R. S., Jarnot, R. F., Pickett, H. M., Read, W. G., Siegel, P. H., Cofield, R. E., Filipiak, M. J., Flower, D. A., Holden, J. R., Lau, G. K., Livesey, N. J., Manney, G. L., Pumphrey, H. C., Santee, M. L., Wu, D. L., Cuddy, D. T., Lay, R. R., Loo, M. S., Perun, V. S., Schwartz, M. J., Stek, P. C., Thurstans, R. P.,

Boyles, M. A., Chandra, K. M., Chavez, M. C., Chen, G.-S., Chudasama, B. V., Dodge, R., Fuller, R. A., Girard, M. A., Jiang, J. H., Jiang, Y., Knosp, B. W., Labelle, R. C., Lam, J. C., Lee, A. K., Miller, D., Oswald, J. E., Patel, N. C., Pukala, D. M., Quintero, O., Scaff, D. M., Vansnyder, W., Tope, M. C., Wagner, P. A., and Walch, M. J.: The Earth Observing System Microwave Limb Sounder (EOS MLS) on the Aura satellite, *IEEE Trans. Geosci. Remote Sens.*, 44, 1075–1092, doi:10.1109/TGRS.2006.873771, 2006. 993

van Gijsel, J. A. E., Swart, D. P. J., Baray, J.-L., Bencherif, H., Claude, H., Fehr, T., Godin-Beekmann, S., Hansen, G. H., Keckhut, P., Leblanc, T., McDermid, I. S., Meijer, Y. J., Nakane, H., Quel, E. J., Stebel, K., Steinbrecht, W., Strawbridge, K. B., Tatarov, B. I., and Wolfram, E. A.: GOMOS ozone profile validation using ground-based and balloon sonde measurements, *Atmos. Chem. Phys.*, 10, 10473–10488, doi:10.5194/acp-10-10473-2010, 2010. 988

Verronen, P. T., Kyrola, E., Tamminen, J., Sofieva, V. F., Clarmann, T., Stiller, G. P., Kaufmann, M., Lopez-Puertas, M., Funke, B., and Bermejo-Pantaleon, D.: A Comparison of Day-time and Night-Time Ozone Profiles from GOMOS and MIPAS, *Envisat Symposium 2007*, 2007. 989

AMTD

8, 987–1011, 2015

GOMOS bright limb data set

S. Tukiainen et al.

[Title Page](#)

[Abstract](#)

[Introduction](#)

[Conclusions](#)

[References](#)

[Tables](#)

[Figures](#)

◀

▶

◀

▶

[Back](#)

[Close](#)

[Full Screen / Esc](#)

[Printer-friendly Version](#)

[Interactive Discussion](#)



**GOMOS bright limb
data set**

S. Tukiainen et al.

Table 1. Wavelength ranges used in the retrieval.

Tangent height range	Wavelength range
> 45 km	280–300 nm, 320–330 nm
40–45 km	300–330 nm, 420–425 nm
< 40 km	420–680 nm

Title Page	
Abstract	Introduction
Conclusions	References
Tables	Figures
◀	▶
◀	▶
Back	Close
Full Screen / Esc	
Printer-friendly Version	
Interactive Discussion	



**GOMOS bright limb
data set**

S. Tukiainen et al.

Table 2. NDACC stations that were used for different latitude zones.

60–90° N	30–60° N	30° S–30° N	30–60° S	60–90° S
Scoresbysund	Obs. de Haute Provence	Paramaribo	Lauder	Dumont d'Urville
Ny Ålesund	Hohenpeißenberg	Izaña		Neumayer
Sodankylä	Legionowo	Natal		
Summit	De Bilt			
Eureka	Boulder			
Alert	Wallops			
Thule	Praha			

[Title Page](#)[Abstract](#)[Introduction](#)[Conclusions](#)[References](#)[Tables](#)[Figures](#)[◀](#)[▶](#)[Back](#)[Close](#)[Full Screen / Esc](#)[Printer-friendly Version](#)[Interactive Discussion](#)

**GOMOS bright limb
data set**

S. Tukiainen et al.

Table 3. Coincidence criteria for the GBL and correlative measurements.

Instrument	Δ_{distance}	Δ_{time}
GOMOS night	250 km	24 h
MLS	200 km	6 h
OSIRIS	200 km	5 h
NDACC sounding	300 km	24 h

**GOMOS bright limb
data set**

S. Tukiainen et al.

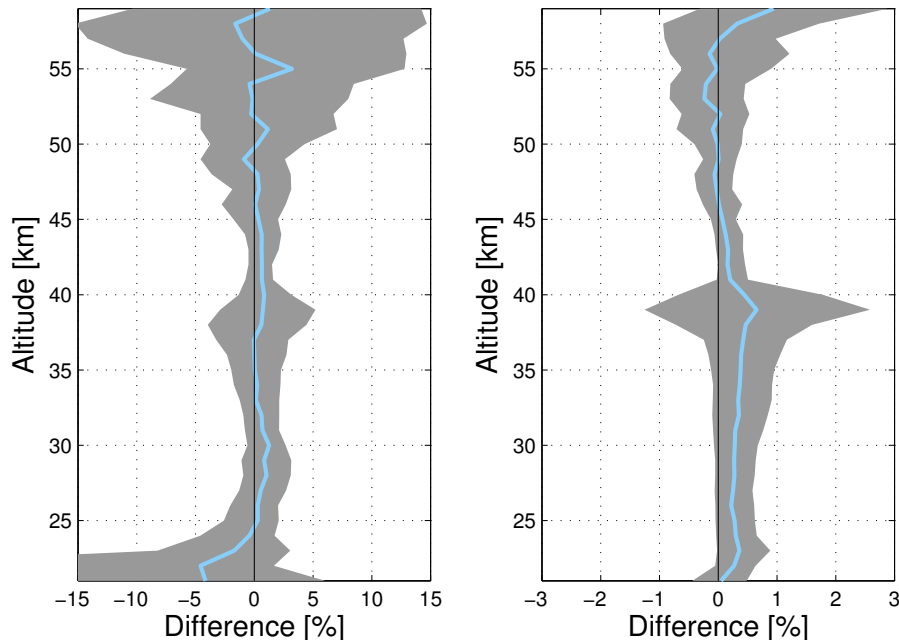


Figure 1. Sensitivity of GBL ozone profile to CCD band (left) and stray light correction method (right). Shown are the mean (solid line) and standard deviation (shaded area) of the relative individual differences of the retrieved profiles in both cases. See text for details.

- [Title Page](#)
- [Abstract](#) [Introduction](#)
- [Conclusions](#) [References](#)
- [Tables](#) [Figures](#)
-
-
- [Full Screen / Esc](#)
- [Printer-friendly Version](#)
- [Interactive Discussion](#)



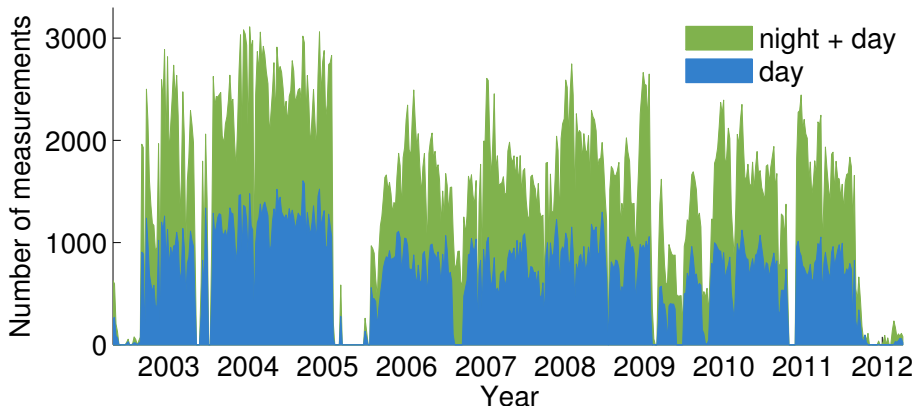


Figure 2. Number of GOMOS night-time and GBL measurements (weekly).

**GOMOS bright limb
data set**

S. Tukiainen et al.

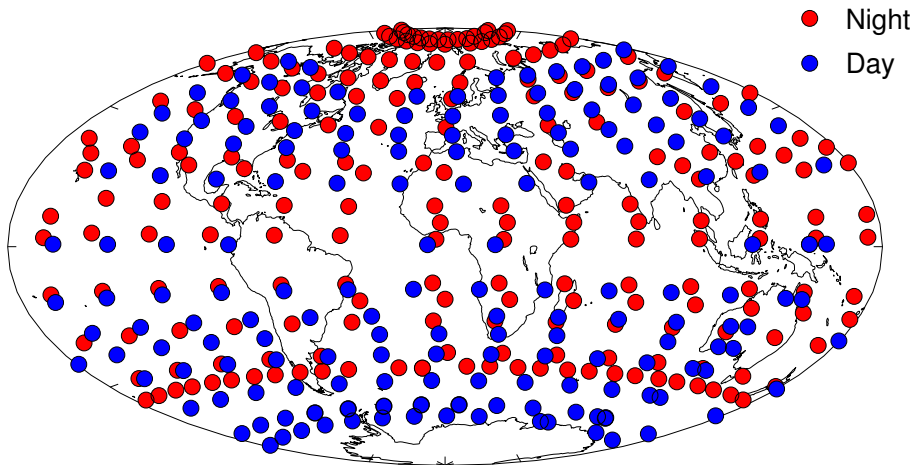


Figure 3. Typical one day coverage of GOMOS night occultations (red) and GBL (blue). Data from 15 December 2004.

[Title Page](#)[Abstract](#)[Introduction](#)[Conclusions](#)[References](#)[Tables](#)[Figures](#)[|◀](#)[▶|](#)[◀](#)[▶](#)[Back](#)[Close](#)[Full Screen / Esc](#)[Printer-friendly Version](#)[Interactive Discussion](#)

**GOMOS bright limb
data set**

S. Tukiainen et al.

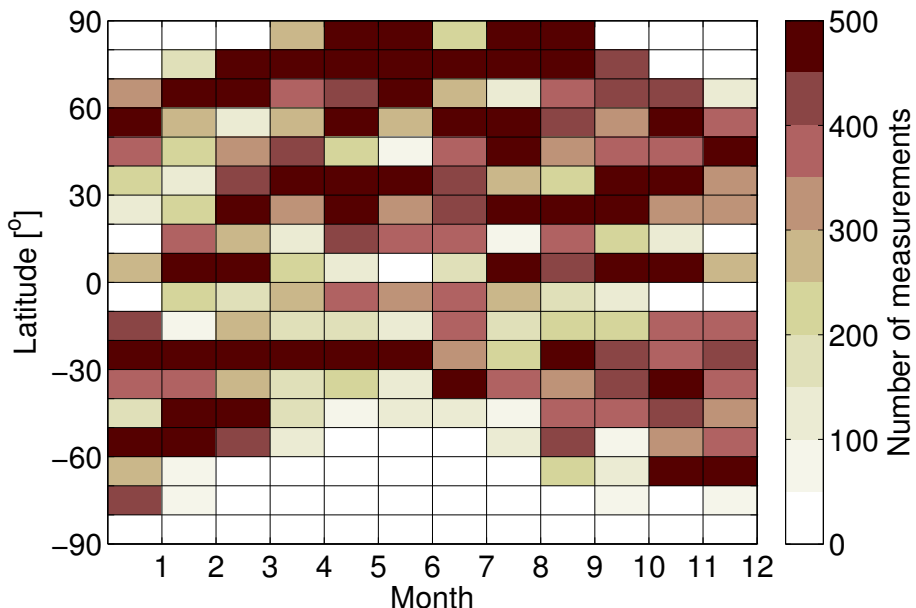


Figure 4. Number of GBL measurements as a function of latitude and time during 2004.

- [Title Page](#)
- [Abstract](#) [Introduction](#)
- [Conclusions](#) [References](#)
- [Tables](#) [Figures](#)
- [◀](#) [▶](#)
- [◀](#) [▶](#)
- [Back](#) [Close](#)
- [Full Screen / Esc](#)

[Printer-friendly Version](#)[Interactive Discussion](#)

**GOMOS bright limb
data set**

S. Tukiainen et al.

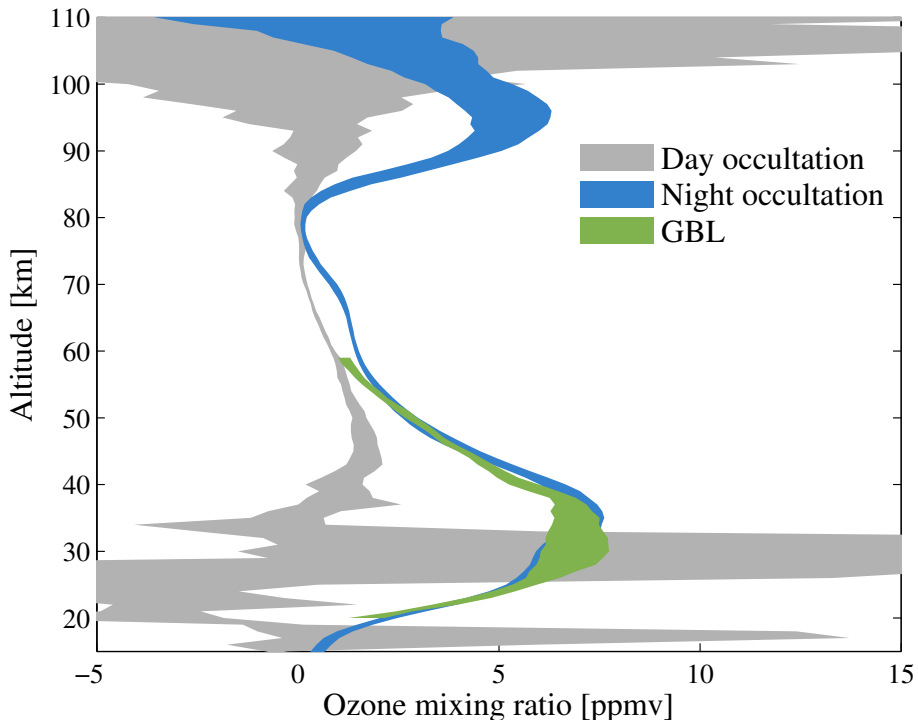


Figure 5. Example of the vertical distribution of ozone from the GOMOS night/day occultations and GBL. Data from January 2005, latitude 35° N (zonal medians and interquartile ranges).

Title Page	Abstract	Introduction
Conclusions	References	
Tables	Figures	
◀	▶	
◀	▶	
Back	Close	
Full Screen / Esc		
	Printer-friendly Version	
	Interactive Discussion	



**GOMOS bright limb
data set**

S. Tukiainen et al.

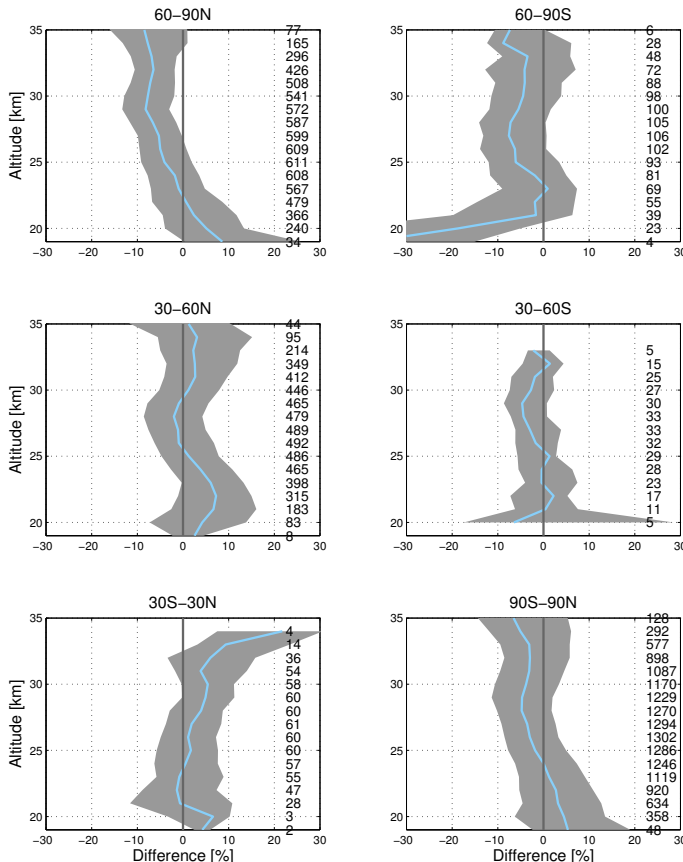


Figure 6. Interquartile ranges (shaded areas) and medians (solid lines) of the individual relative differences of GBL ozone profiles against NDACC ozone soundings for different latitude zones. The numbers are the amount of co-located points at each tangent height.

Title Page	Abstract	Introduction
Conclusions	References	
Tables	Figures	
		
Back	Close	
Full Screen / Esc		
Printer-friendly Version		
Interactive Discussion		



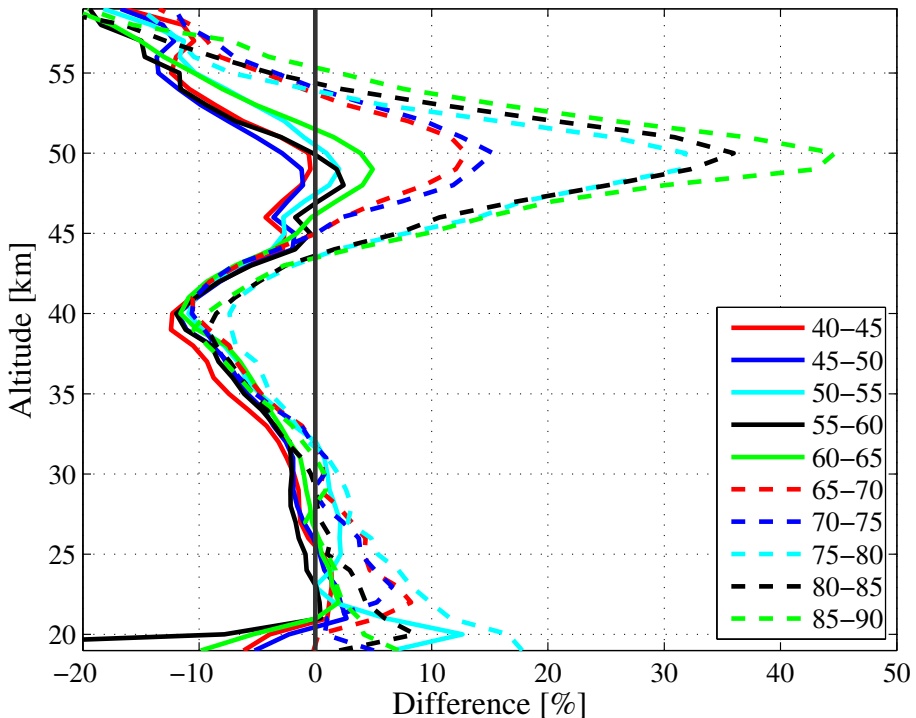


Figure 7. Median relative differences of GBL ozone profiles against GOMOS night-time occultations for different solar zenith angles.

**GOMOS bright limb
data set**

S. Tukiainen et al.

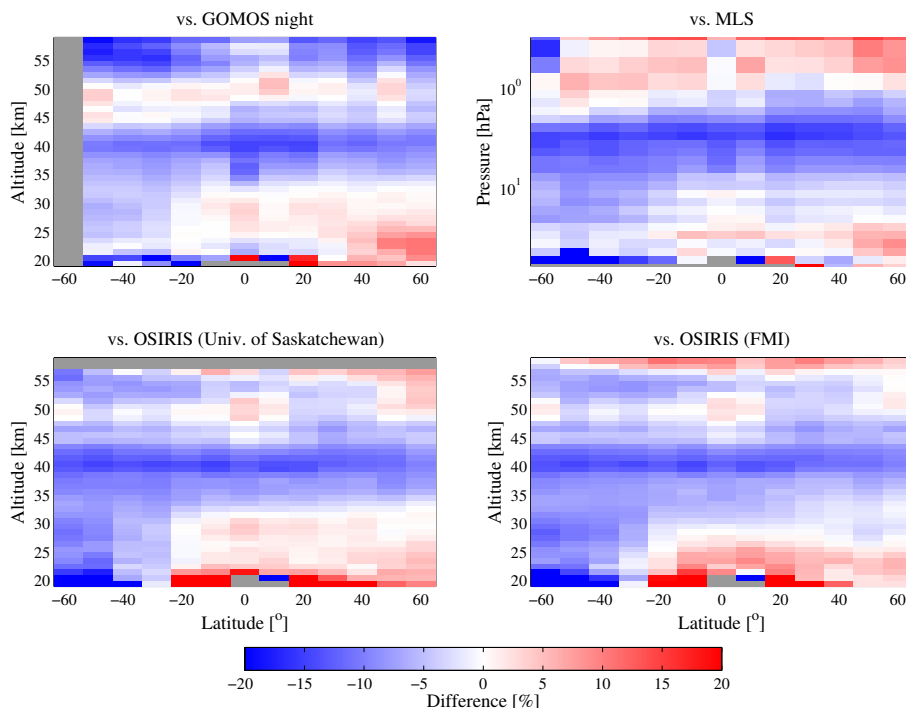


Figure 8. Median relative differences of GBL ozone profiles against GOMOS night-time occultations (upper left), MLS (upper right), OSIRIS University of Saskatoon version (lower left), and OSIRIS FMI version (lower right).